

SUPPLEMENTARY FIGURE CAPTIONS

Figure DR1. A: Satellite image of Otog Mesa and parallel trough to the east (from bing.com/map). The geomorphically-effective wind direction is shown by the red arrow. Linear wind-parallel ridges and valleys are present on both the upwind and downwind sides of Otog Mesa. Development of the mesa-parallel Otog trough is attributed to wind scour. Downwind of the Otog Trough are sand dunes that sit at higher elevation. B: Satellite image of yardangs in Cretaceous strata along the northwestern margin of Otog Mesa (from bing.com/map). Red arrows show geomorphically-effective wind directions.

Figure DR2. Google Earth images showing the variable orientation and expression of linear loess topography across the Loess Plateau where it is prominent and ubiquitous (A-D) and spatially patchy and/or more cryptic but still resolvable (E-G). F-H also shows the clockwise rotation in linear loess topography orientation over distances of <10 km. Red arrows show the dominant orientation of the linear loess topography.

Figure DR 3. Rose diagrams of orientation measurements from $\sim 1^\circ \times 1^\circ$ areas outlined in the black boxes. Mean azimuth values and their standard deviations are indicated where orientations are unimodal.

Figure DR4. Mean (from 1979-2010) near-surface (10 m height) wind vectors during A: spring, B: summer, C: fall, and D: winter. Near-surface (10 m height) wind vectors averaged over a 6-hour time period of maximum wind speed during documented dust storms: E: March 19, 2010 (Ling et al., 2011); F: March 27, 1985 (Song et al., 2009); and G: March 15, 1999 (Liu et al., 2004). Data are from the National Oceanic and Atmospheric Administration's Climate Forecast System Reanalysis (Saha et al., 2010).

REFERENCES CITED

- Ling, X.-L., Guo, W.-D., Zhao, Q.-F., and Zhang, B.-D., 2011, A case study of a typical dust storm event over the Loess Plateau of northwest China: Atmospheric and Oceanic Science Letters, v. 4, p. 344-348.
- Liu, L.Y., Shi, P.J., Gao, S.Y., Zou, X.Y., Erdon, H., Yan, P., Li, X.Y., Ta, W.Q., Wang, J.H., and Zhang, C.L., 2004, Dustfall in China's western loess plateau as influenced by dust storm and haze events: Atmospheric Environment, v. 38, p. 1699-1703.
- Saha, S., et al., 2010, The NCEP Climate Forecast System Reanalysis: American Meteorological Society, v. 91, p. 1015-1057.
- Song, M.H., Qian, Z.A., Cai, Y., and Liu, C.M., 2009, Analyses of spring mean circulations for major and minor dust storm years in China-Mongolia area: Sciences in Cold and Arid Regions, v. 1, p. 361-371.

Figure DR1A

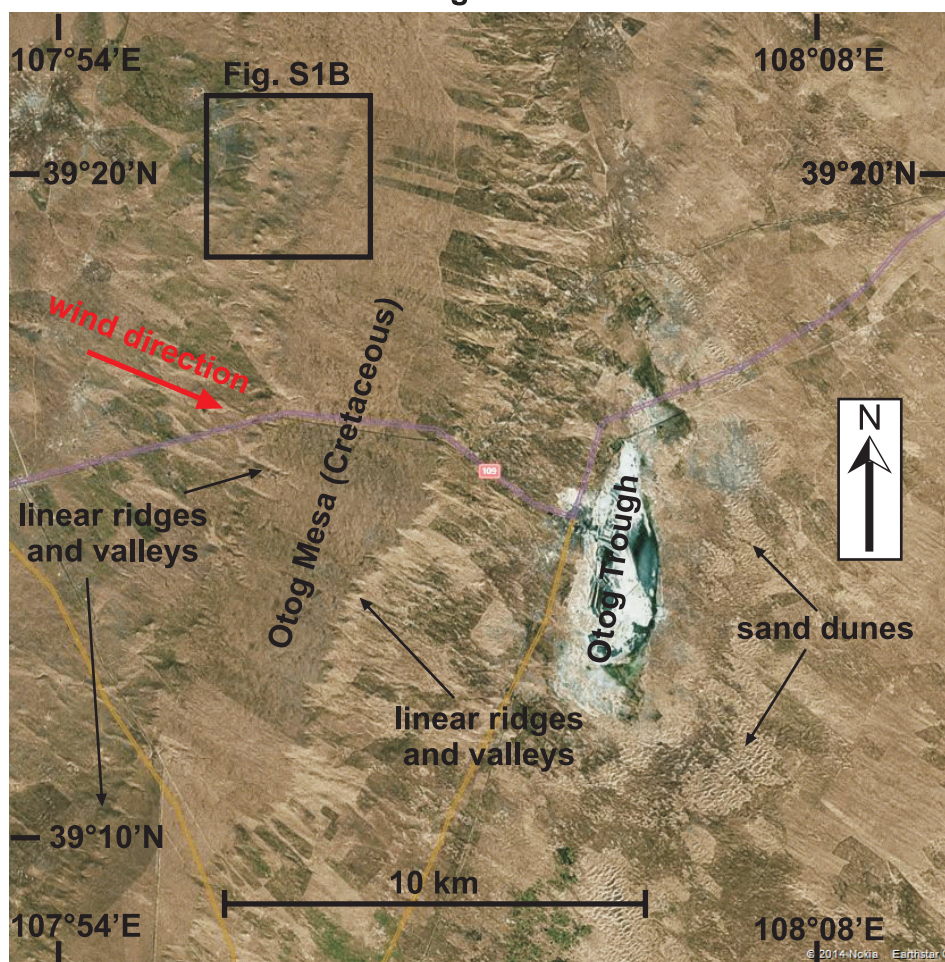


Figure DR1B

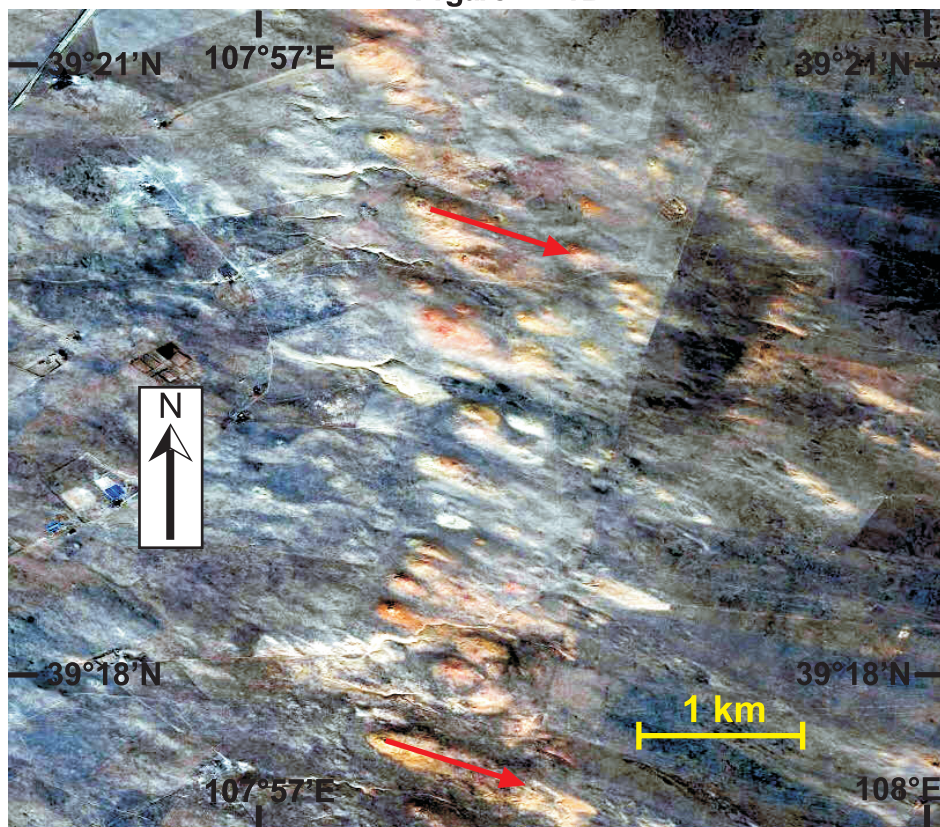


Figure DR2A

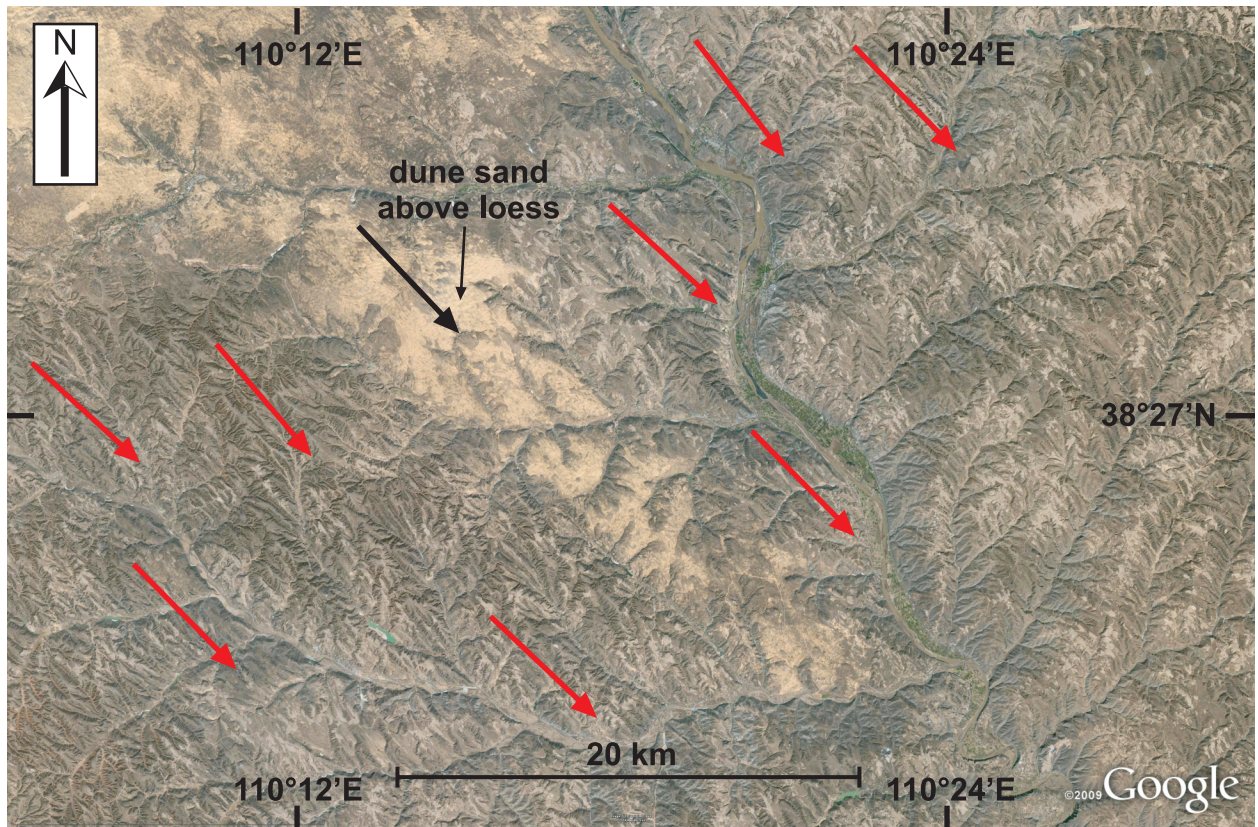


Figure DR2B

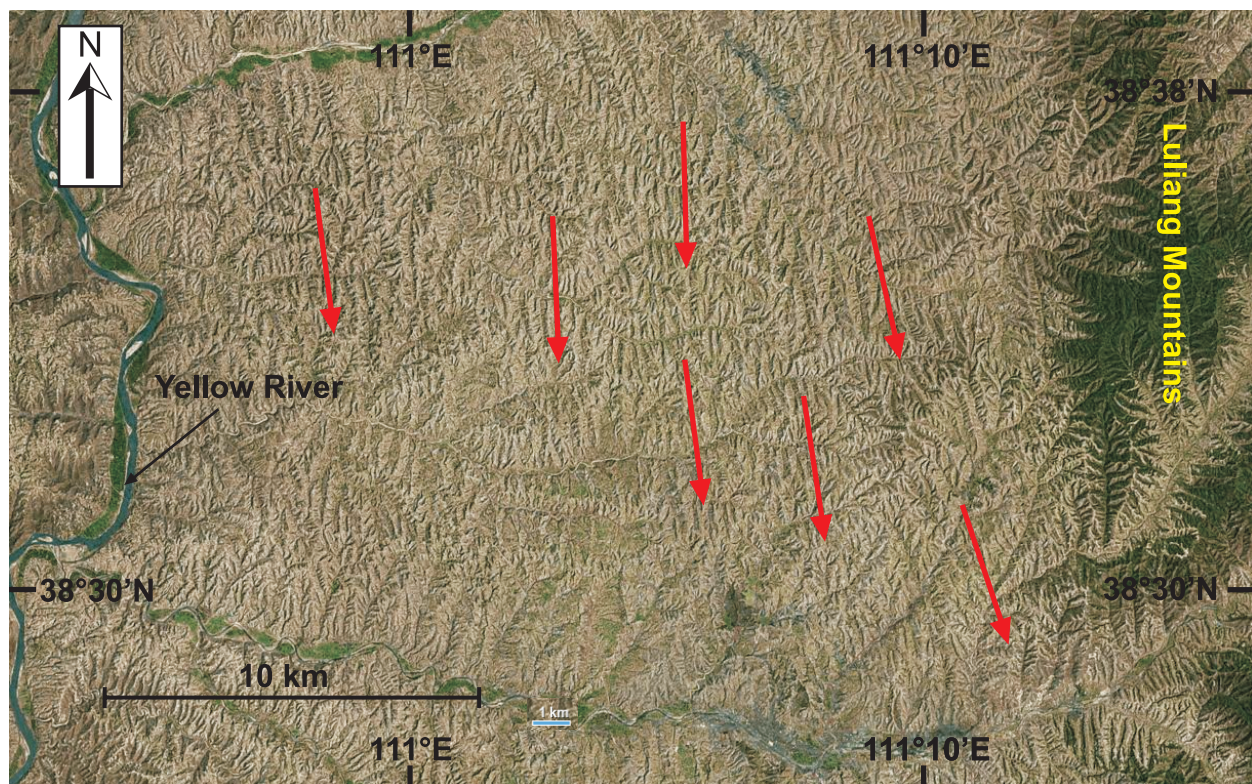


Figure DR2C

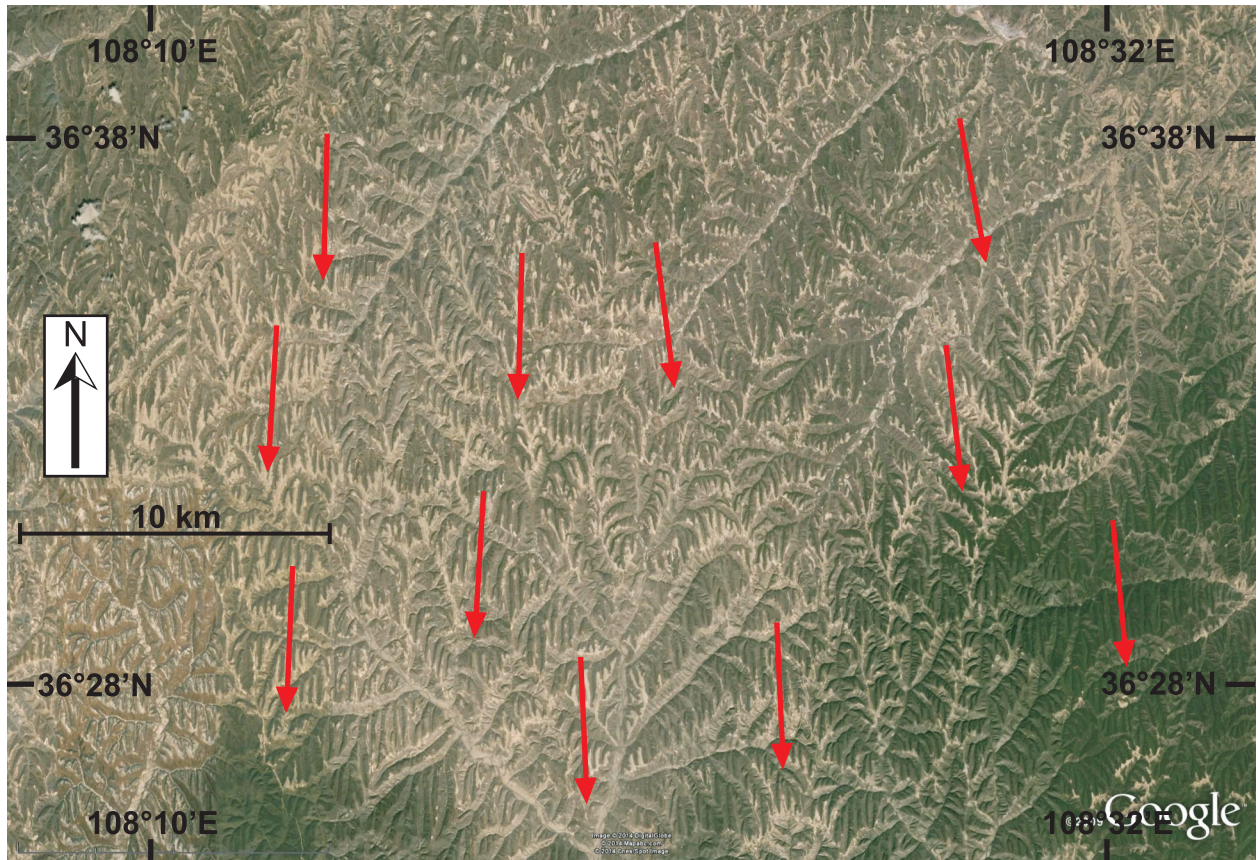


Figure DR2D

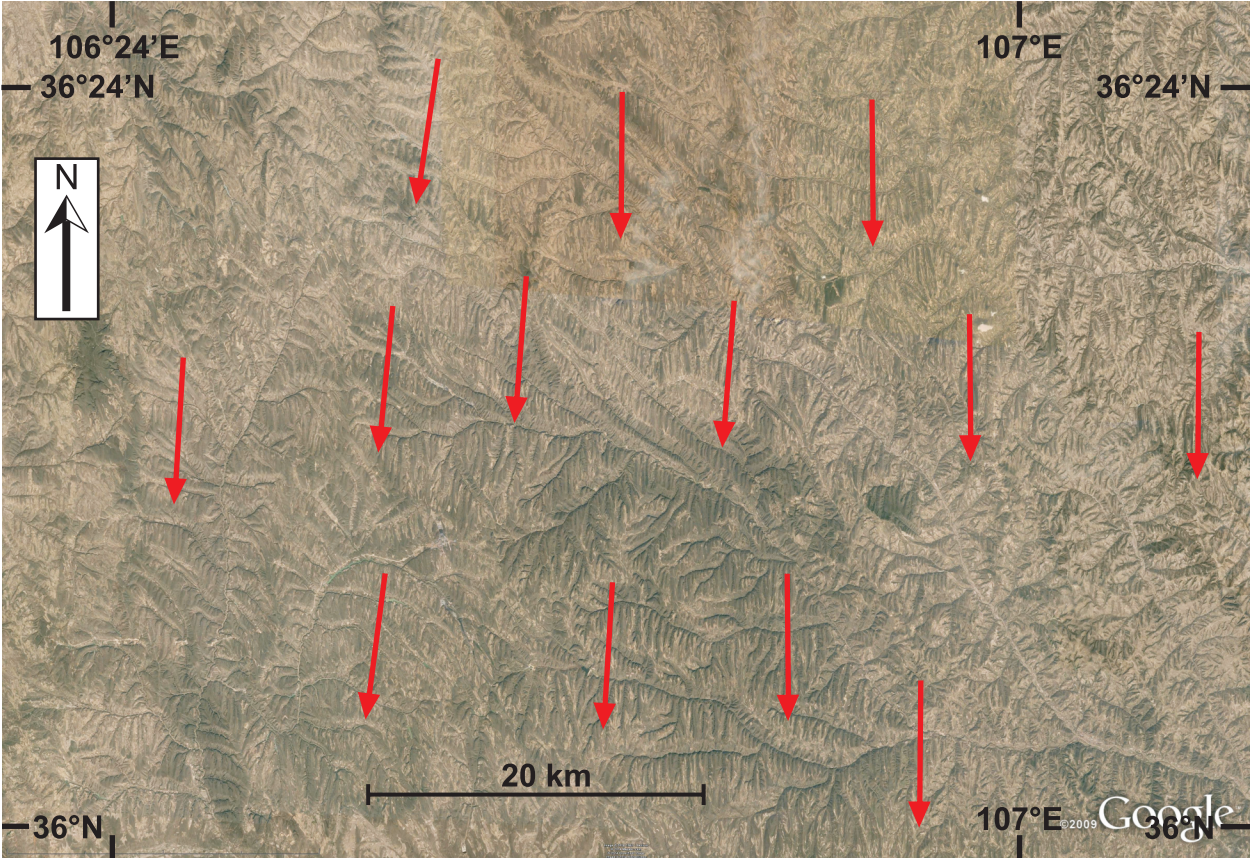


Figure DR2E

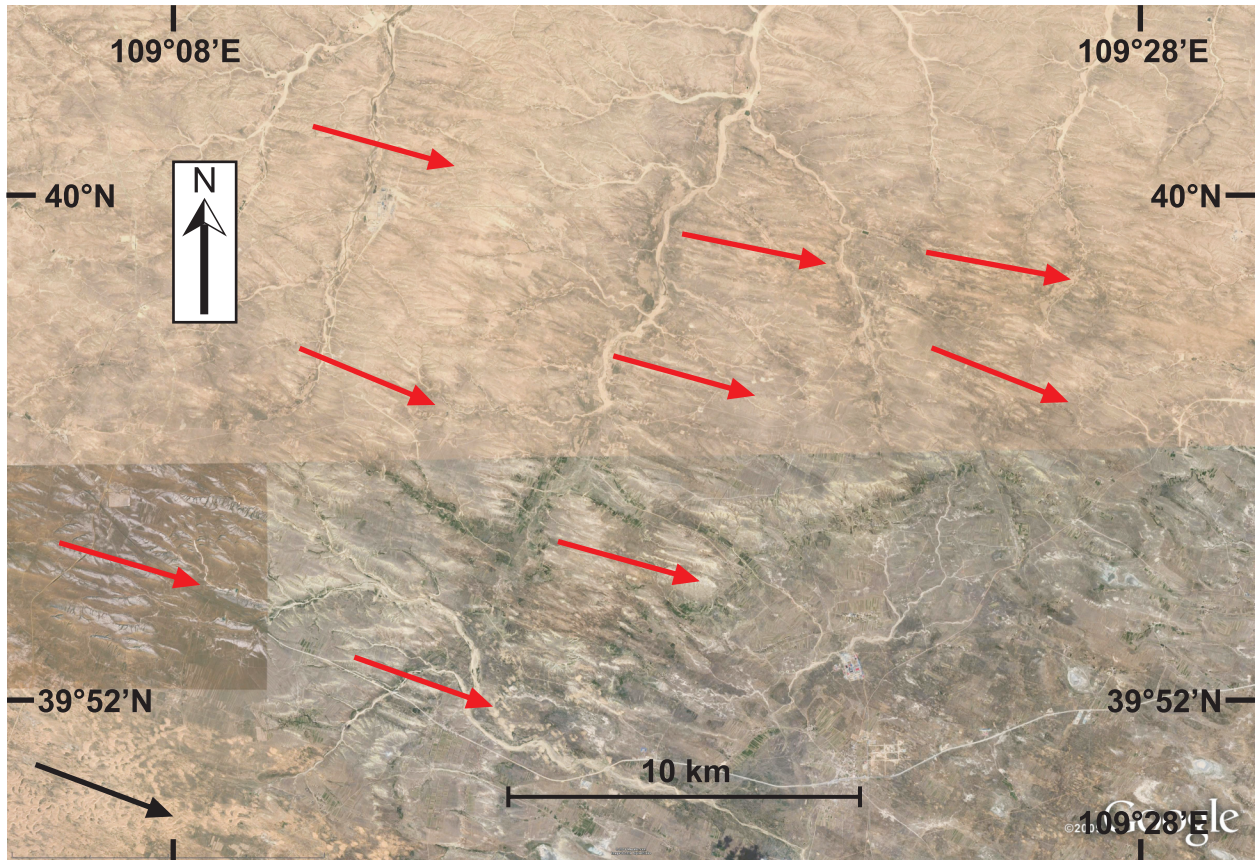


Figure DR2F

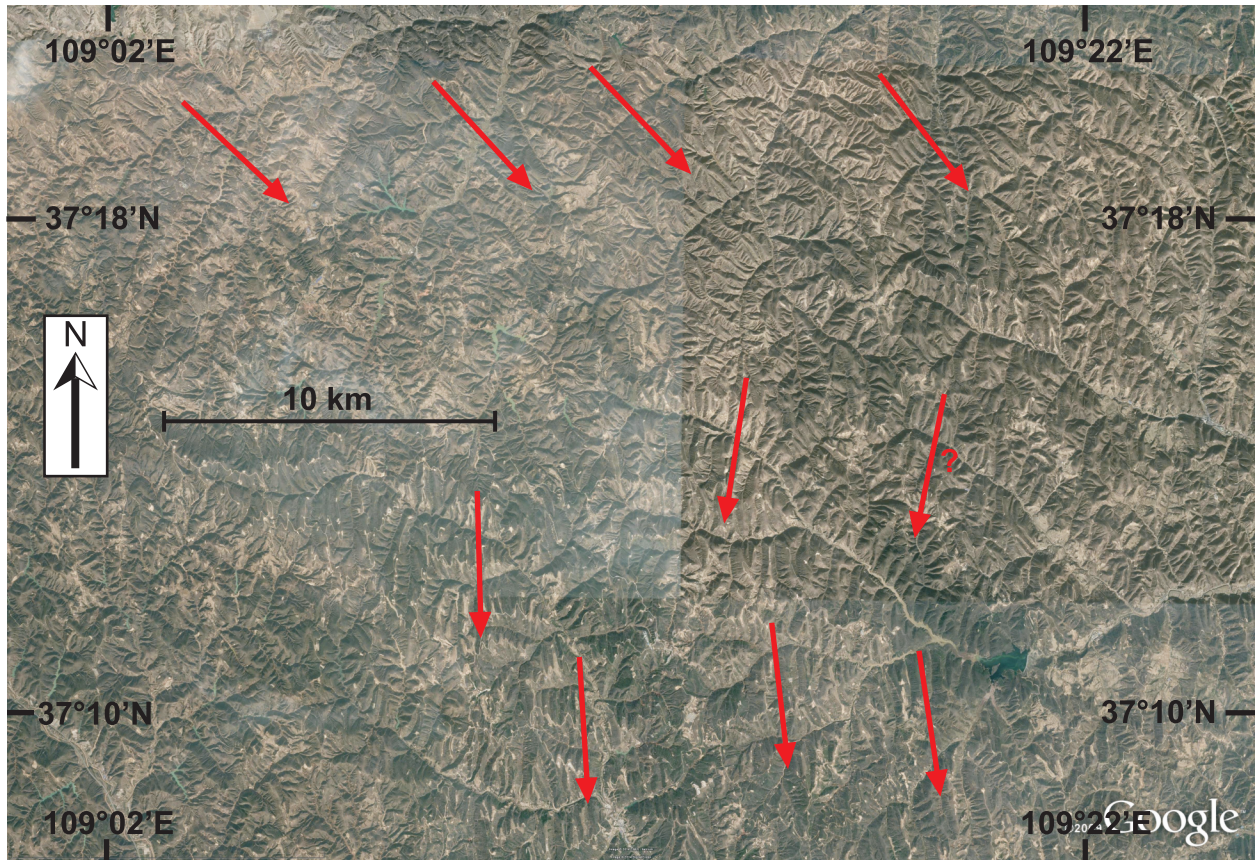


Figure DR2G

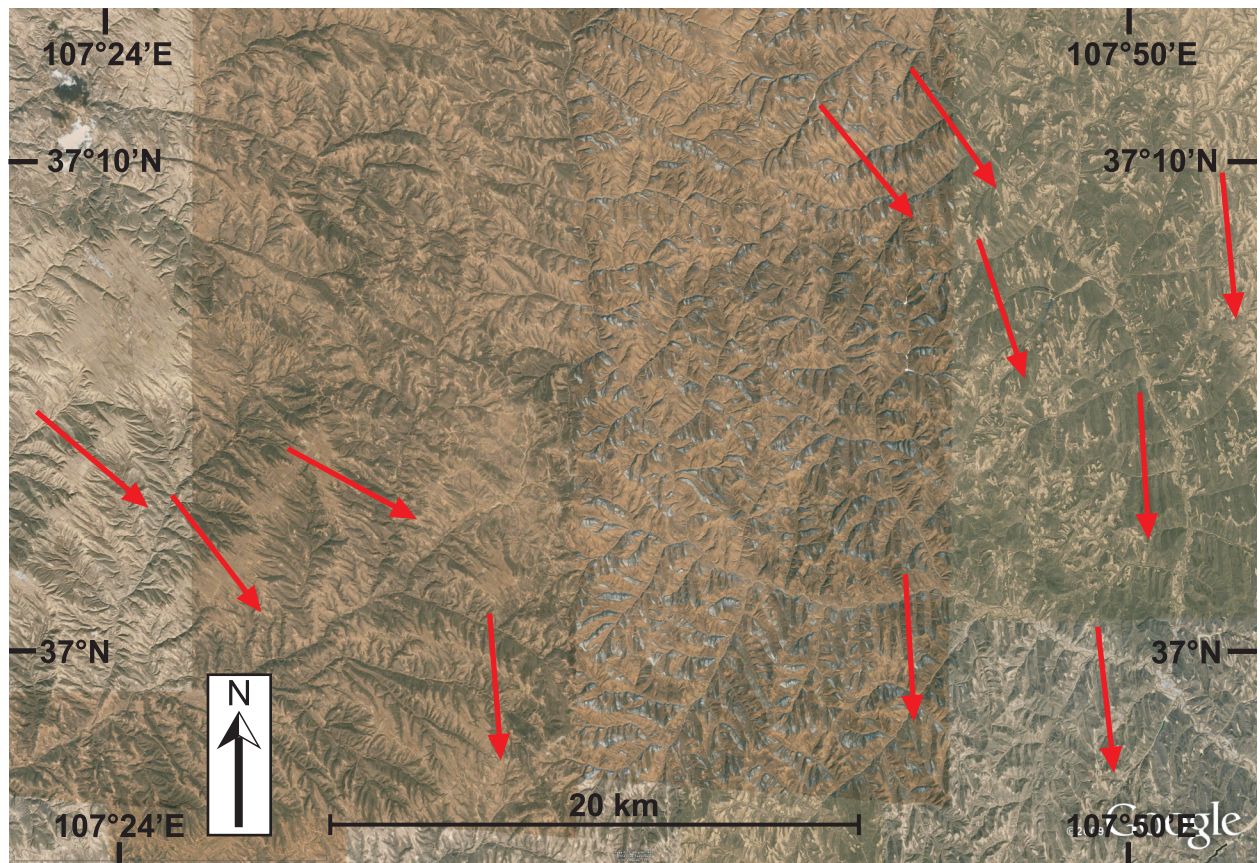


Figure DR2H

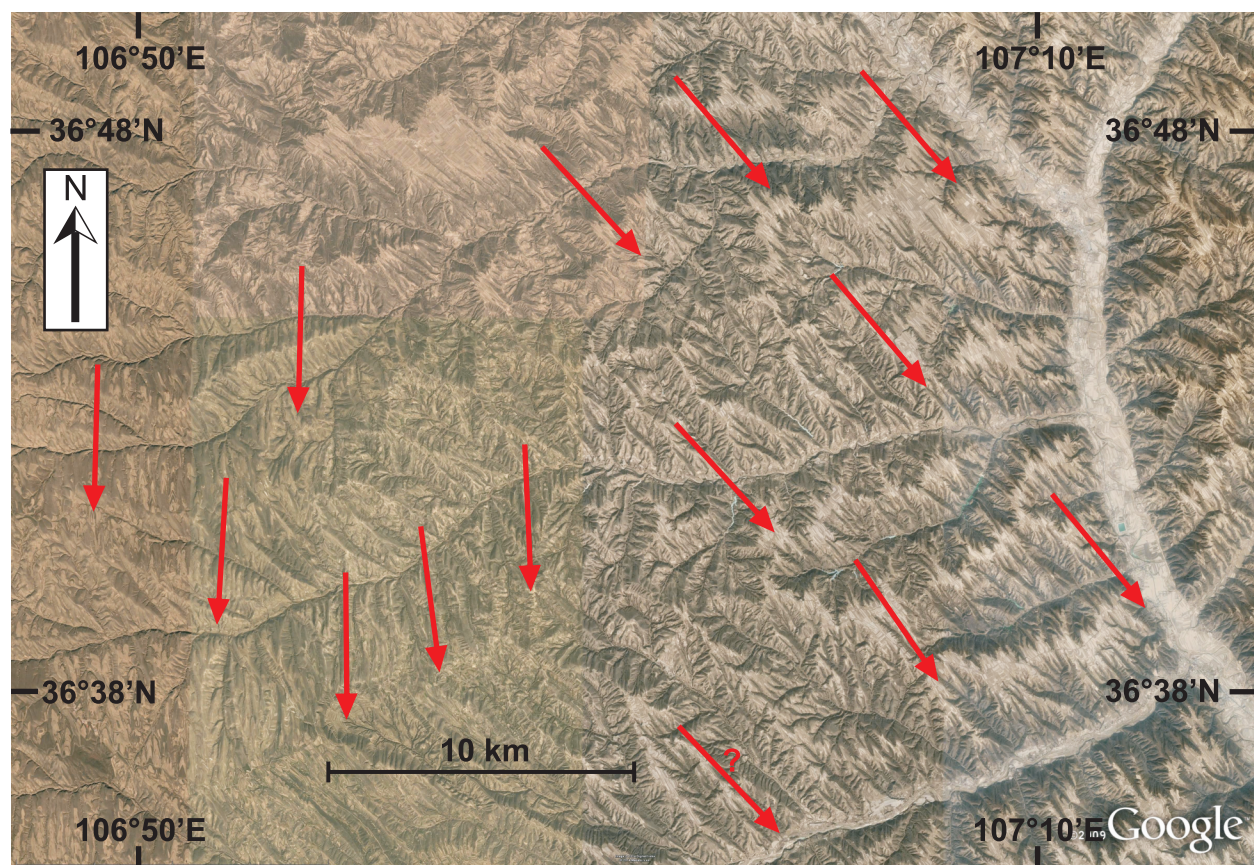


Figure DR3

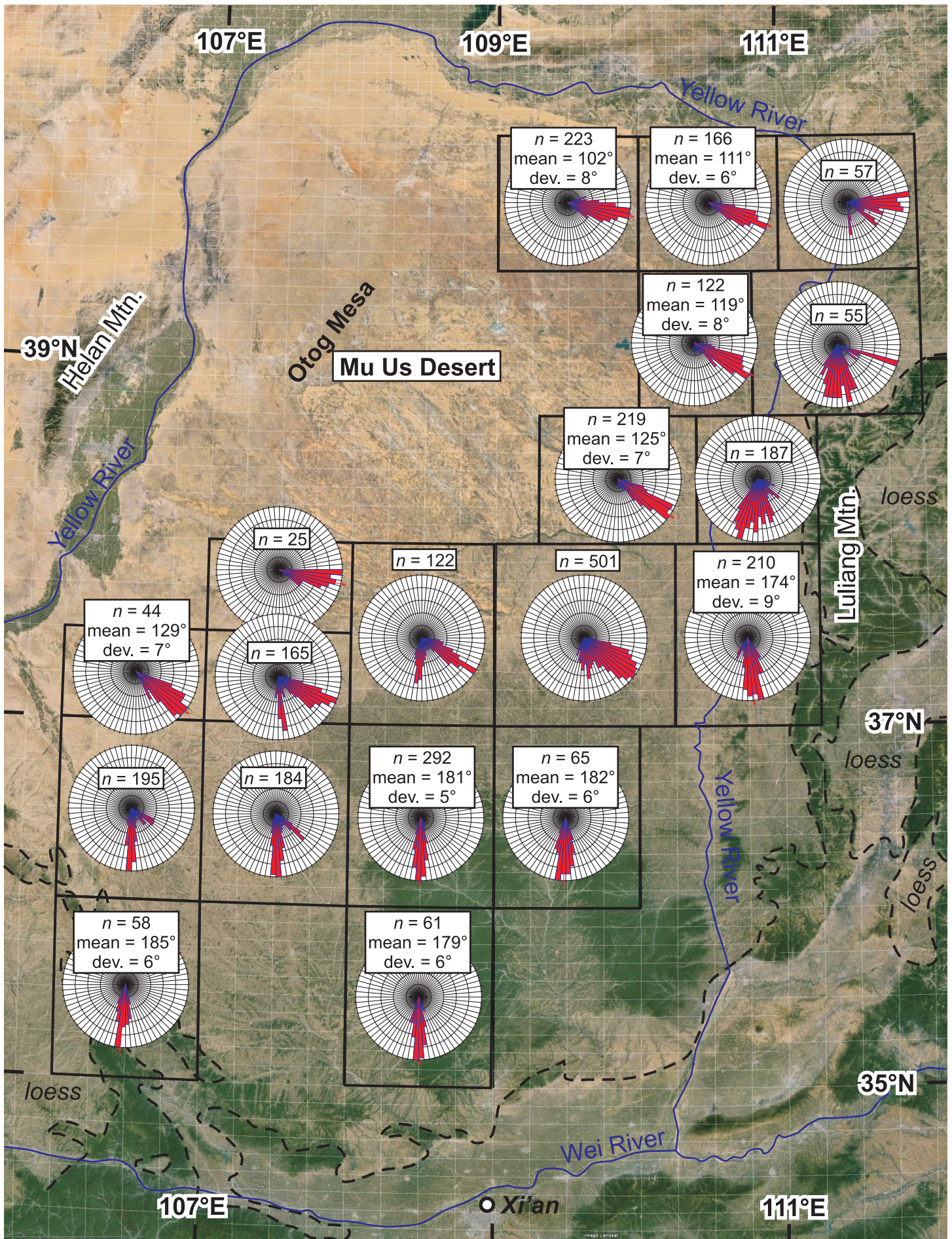


Figure DR4A

Mean Spring (March-April-May, 1979-2010)

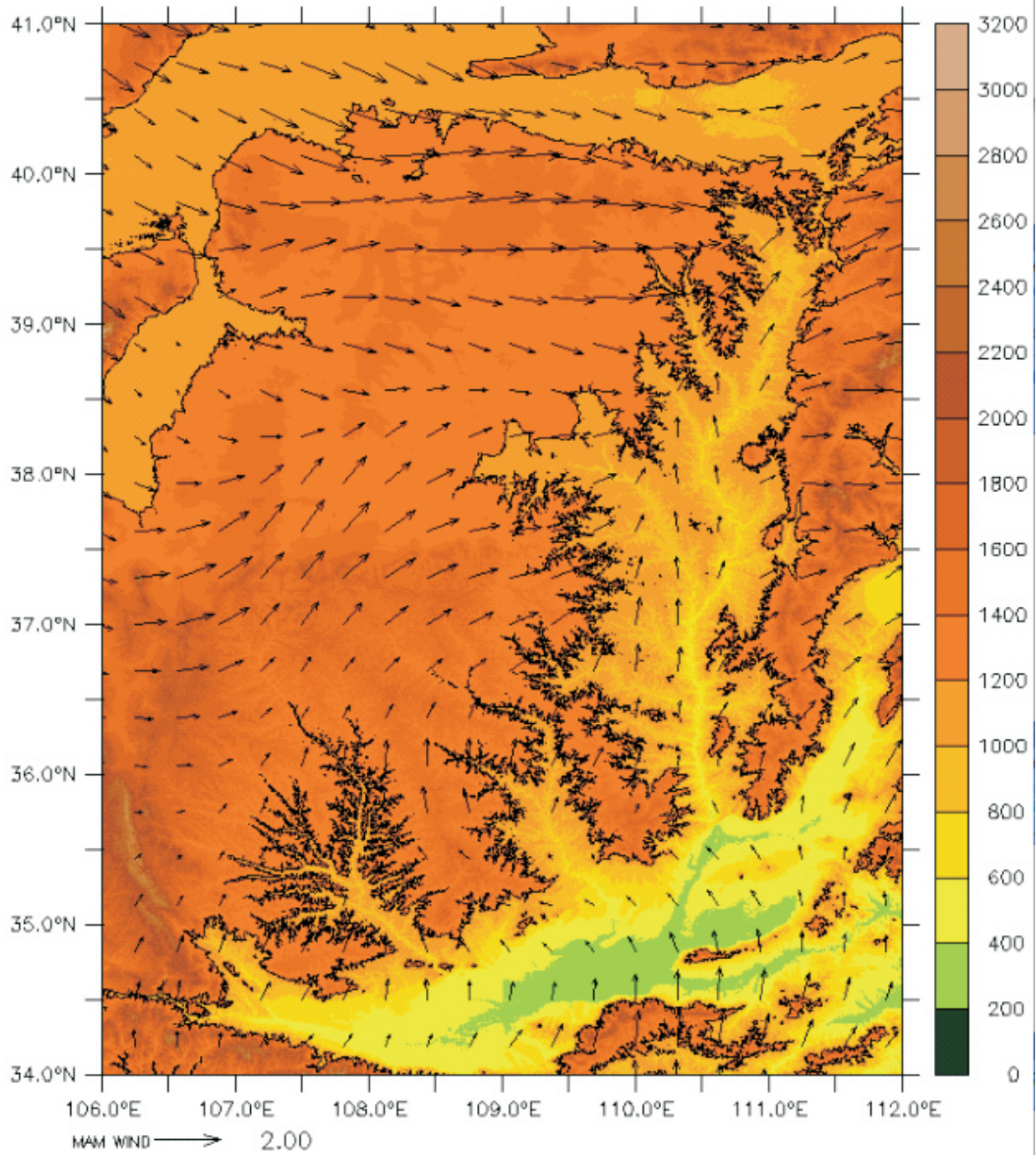


Figure DR4B

Mean Summer (June-July-August, 1979-2010)

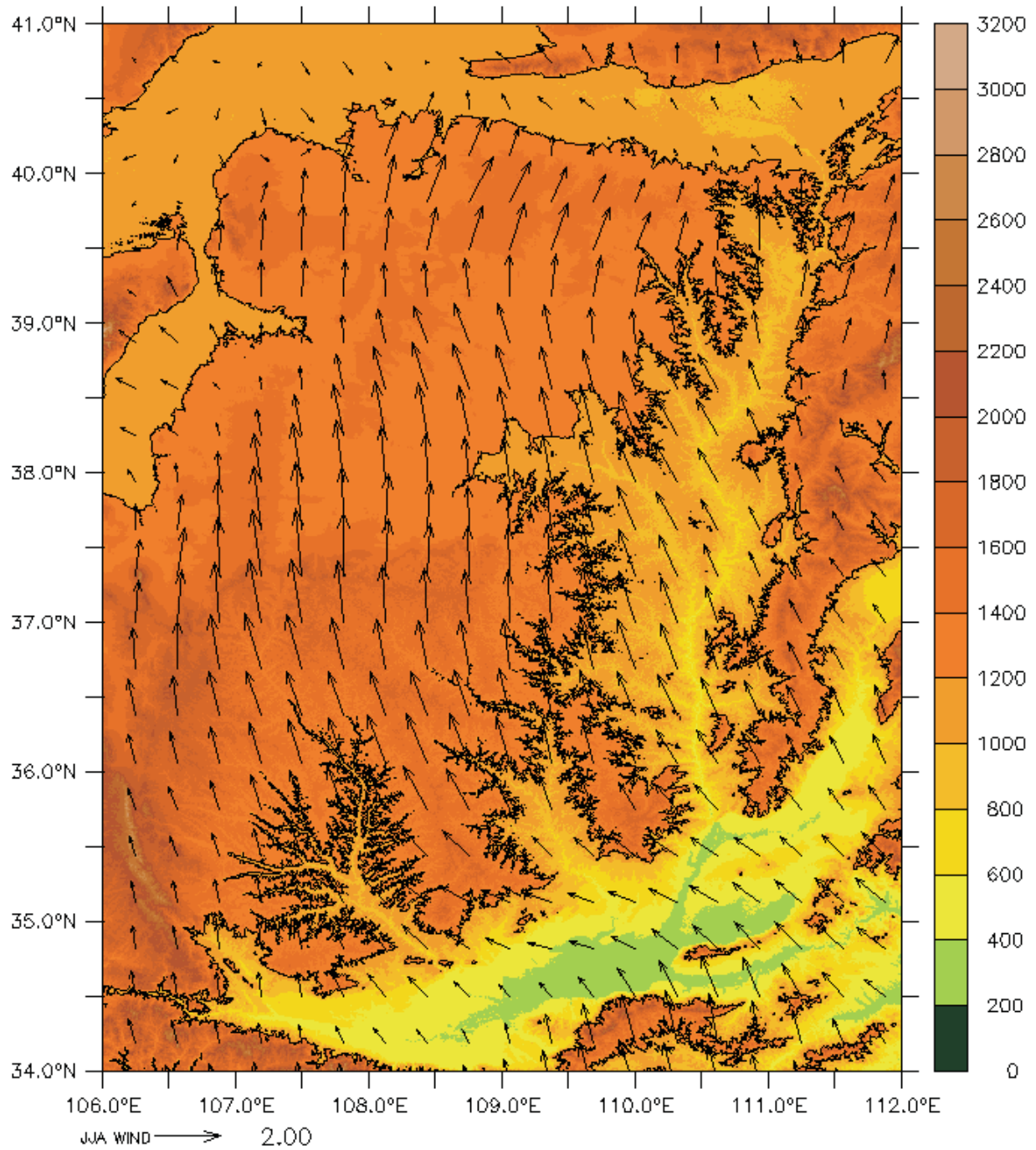


Figure DR4C

Mean Fall (September-October-November, 1979-2010)

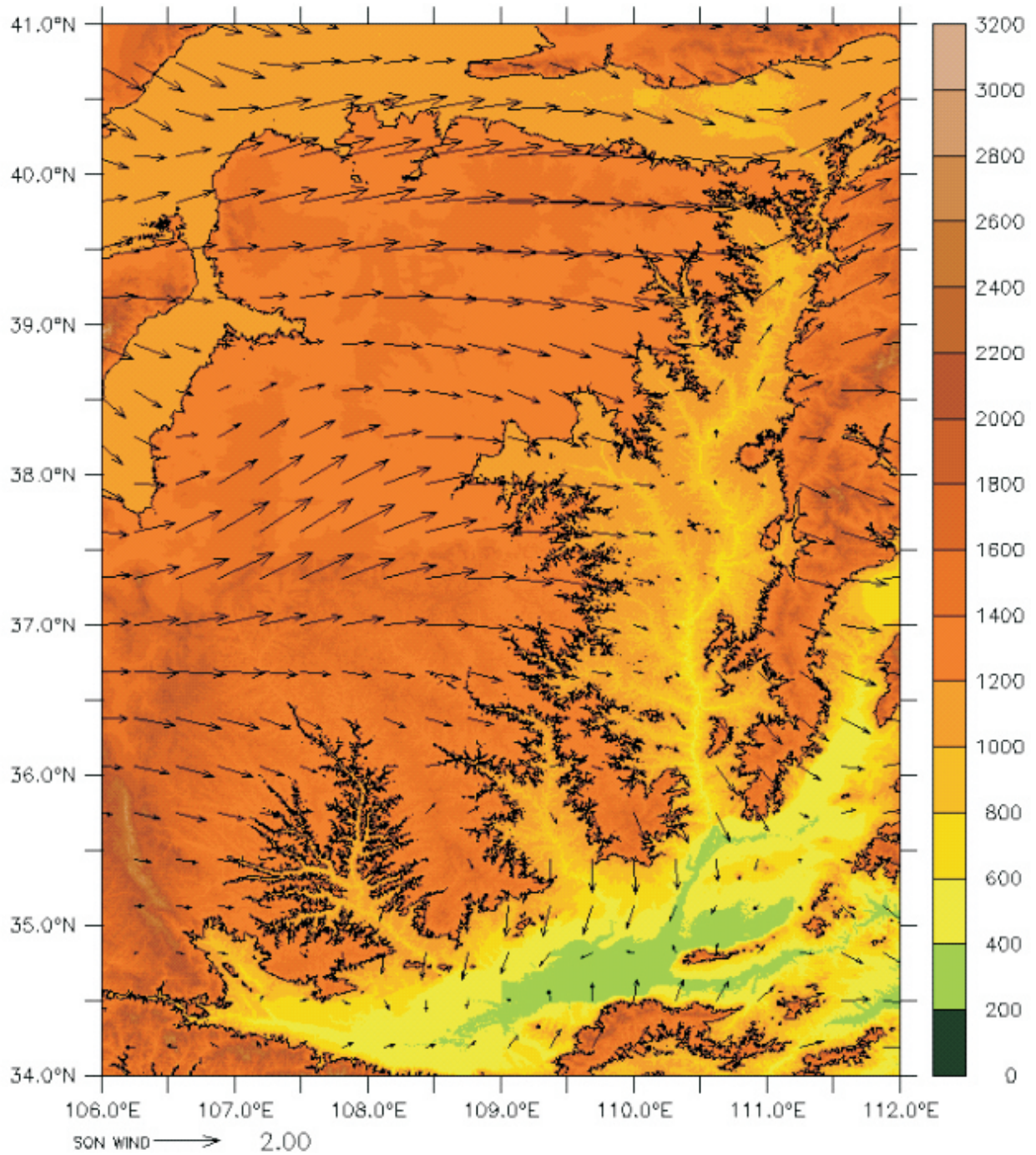


Figure DR4D

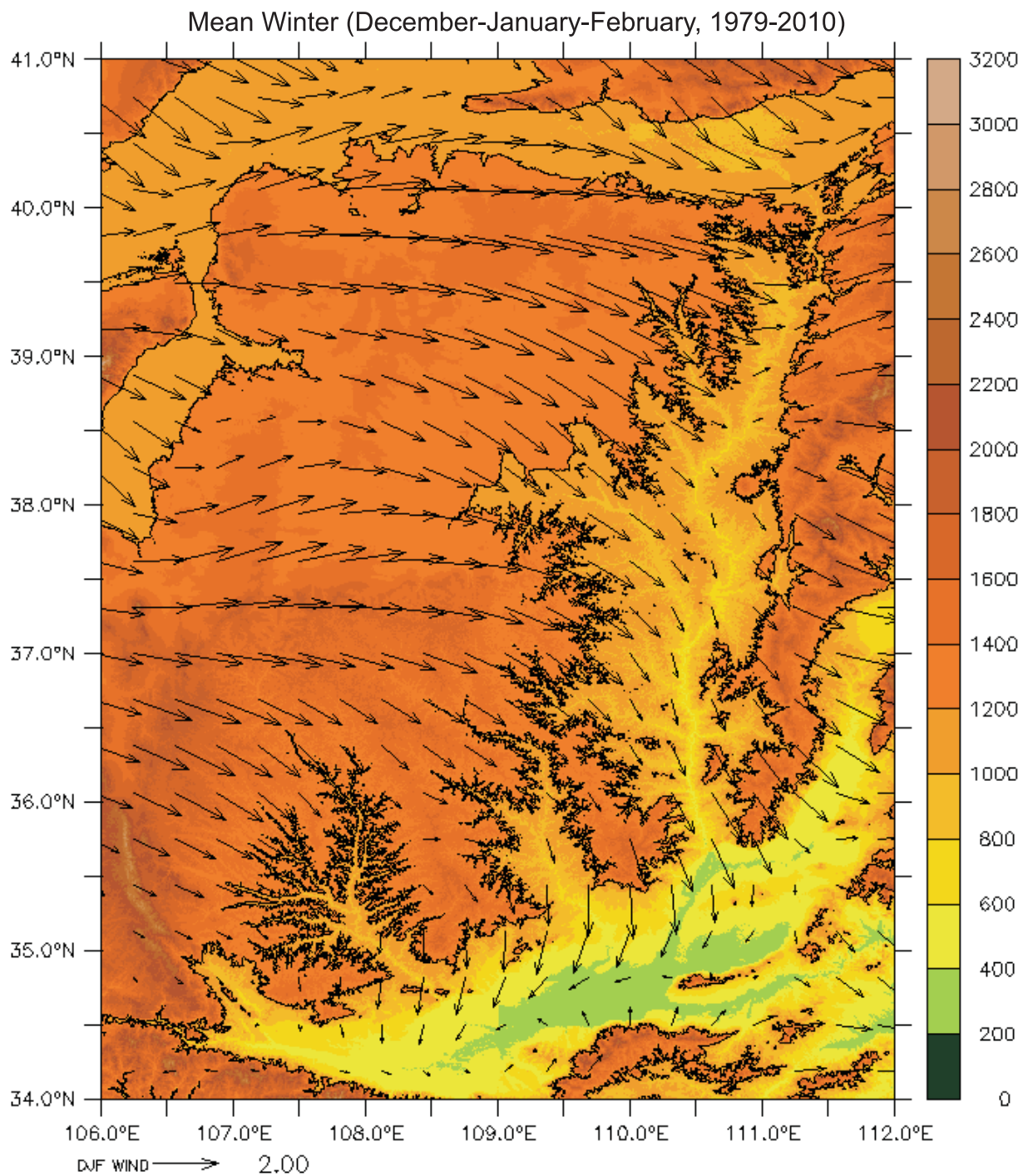


Figure DR4E

March 19, 2010 wind storm

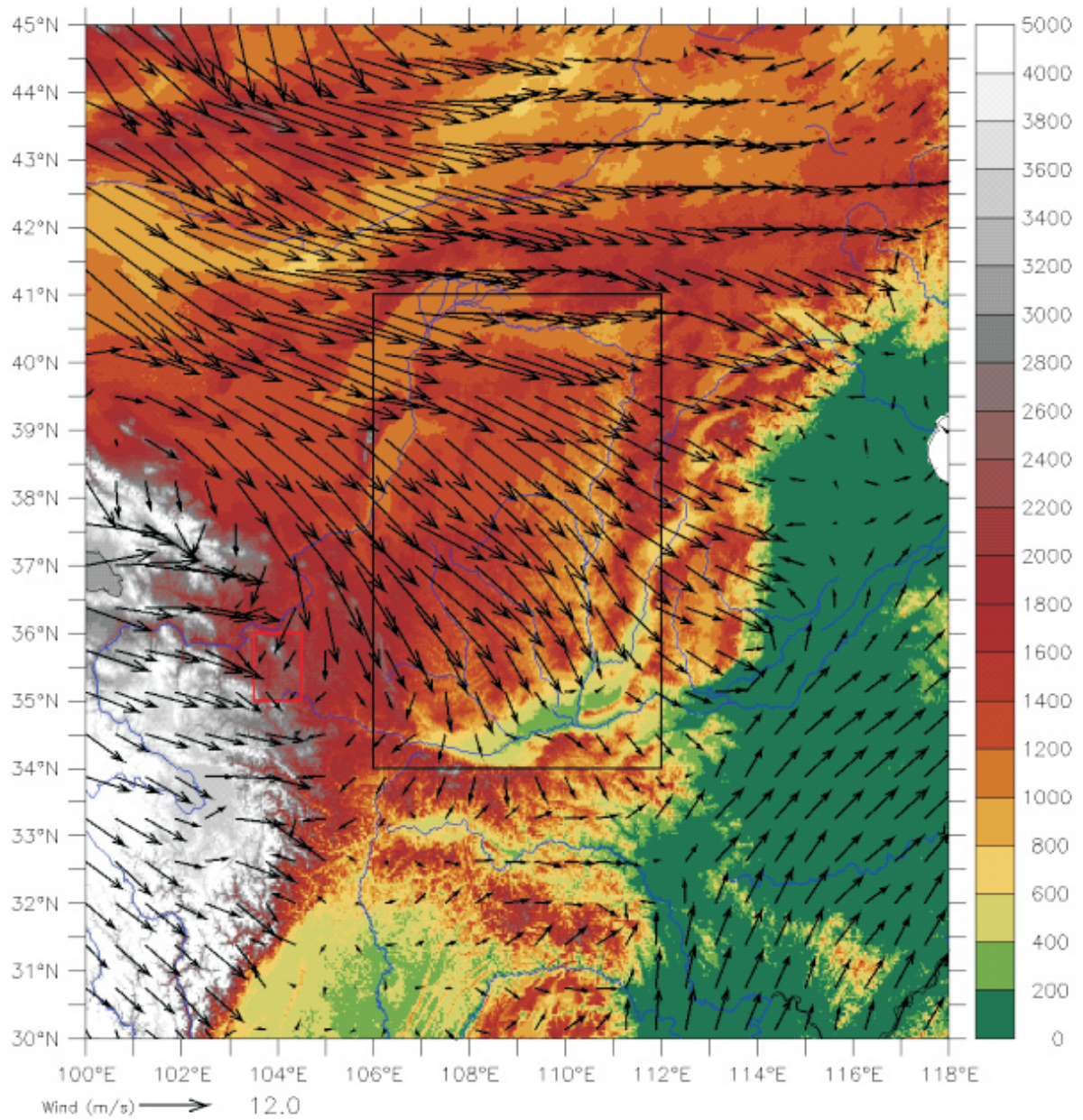


Figure DR4F

March 27, 1985 wind storm

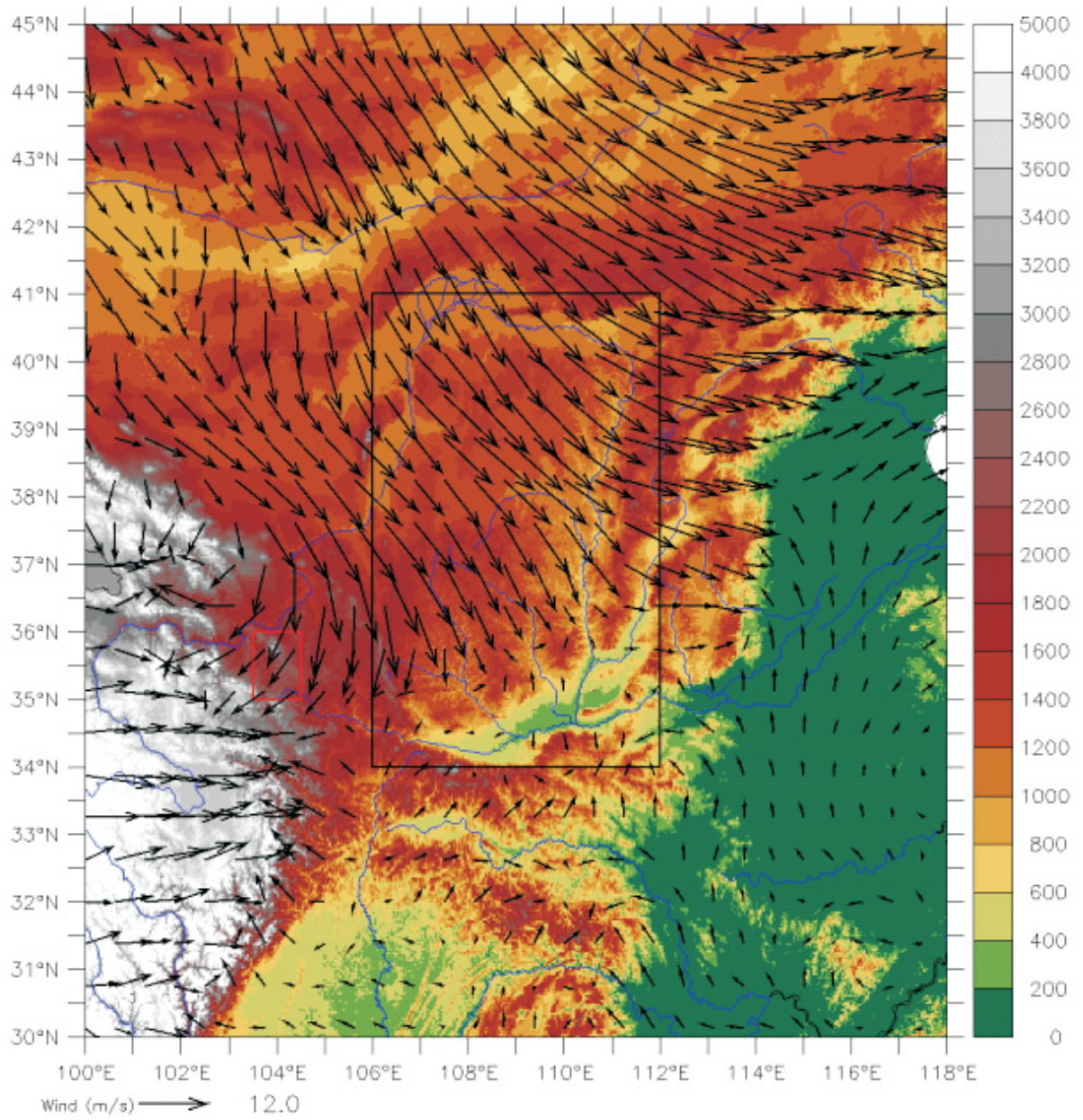


Figure DR4G

March 15, 1999 wind storm

